Chapter 1

Nanoscale Biosensor for Detection of Reactive Oxygen Species

Tarl W. Prow, Daniel Sundh, and Gerard A. Lutty

Abstract

Noninvasive detection of biological responses to reactive oxygen species (ROS) in vivo could shed light on mechanisms at work in diverse areas like developmental dynamics, therapeutic effectiveness, drug discovery, pathogenic processes, and disease prevention. Research on ROS is usually dependent on in vitro models without translational relevance. Nanoscale (<100 nm) particulates are attractive carriers and platforms for biosensor technology due to their small size, flexible assembly, and favorable toxicity profiles. Intracellular signalling pathways activated in response to ROS have been well documented and mechanisms elaborated. Likewise, there is a wealth of genetic reporter systems that utilize fluorescent proteins capable of being monitored noninvasively. We combined these elements into a platform technology that utilizes nanoparticle-tethered synthetic genetic elements that respond to cellular response elements to report endogenous responses to oxidative insult through fluorescent gene expression. We envision the future of this technology to play a research role quantifying oxidative stress in vivo and a future clinical role as an automated theragnostic for ROS-related diseases. The production of this nanobiosensor technology utilizes off-the-shelf components and can be carried out in a molecular biology laboratory. Assessment of fluorescent protein expression can be done with noninvasive imaging and quantitative protein expression analysis. This is a flexible nanoparticle-based reporter system for monitoring in vivo responses to ROS.

Key words Magnetic nanoparticles, Reactive oxygen species, Non-invasive imaging, Antioxidant response element

1 Introduction

Some common nanoparticles for human use are ZnO/TiO_2 in sunscreens [1, 2], colloidal silver for wound healing and antimicrobial uses [1], and magnetic nanoparticles (MNPs) used as contrast agents [3]. Clinically, magnetic resonance imaging utilizing MNP relies on the MNP to accelerate the relaxation rate of nearby water molecules after a magnetic field pulse. In the laboratory, MNPs have been developed for cell separation applications. Decades of clinical use show that ultrasmall superparamagnetic iron oxide injected intravenously is safe [4]. Magnetic-activated cell sorting

Donald Armstrong and Dhruba J. Bharali (eds.), *Oxidative Stress and Nanotechnology: Methods and Protocols*, Methods in Molecular Biology, vol. 1028, DOI 10.1007/978-1-62703-475-3_1,

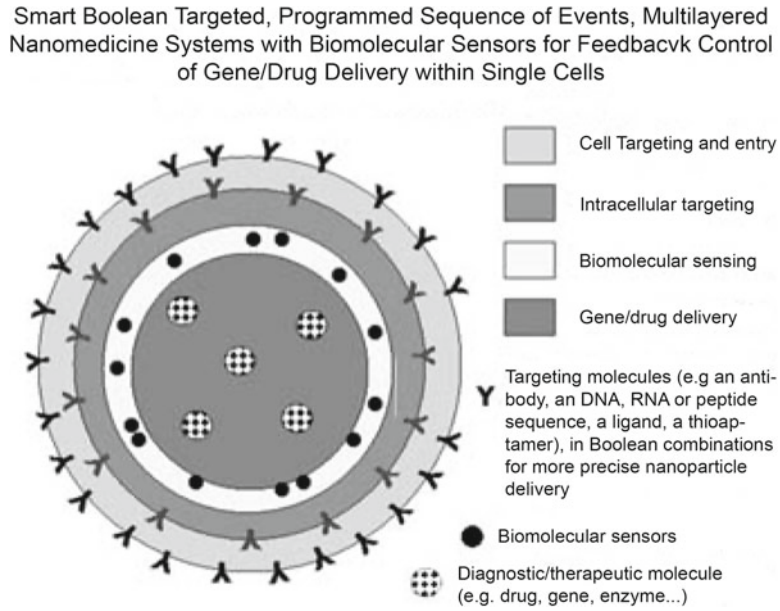

Fig. 1 Schematic image of a smart nanoparticle system that can produce an ordered series of events for drug/gene delivery (Prow et al. (2004) J Mol Histol;35:555–564)

has proved to be nontoxic and had a significant impact on stem cell [5] and immunology [6] research in recent decades. There are a wide variety of MNP products available for purchase. The relative ease of preparation and conjugation of surface molecules has led to the commercialization of MNP with fluorescent, antibody, and/or streptavidin moieties displayed on the MNP surface from a variety of manufactures. The streptavidin and amine surfaces are of direct relevance to our MNP-ROS biosensor application. These MNPs can be coupled to biotin or other labeled PCR products. We started using MNP primarily because of the safety profiles generated by years of contrast agent use. The fact that there are now a selection of sizes and surface chemistries further supports the use of MNP as in vivo research tools. We have successfully used streptavidin-coated nanoparticles (Fig. 3) for in vitro antibody and peptide targeting [7], in vitro gene delivery [8, 9], in vivo toxicology [10, 11] and in vivo biosensor delivery coupled with reactive oxygen species (ROS) monitoring [12] (Figs. 1 and 2). These studies were done with a primary focus on ocular applications, but MNP-tethered antioxidant response elements (ARE) could be used for a variety of models and offer a unique set of advantages that form the framework for this novel biosensor technology.

ROS and resultant oxidative stress has been implicated in a variety of disease states, including diabetes [13–16] and age-related macular degeneration (AMD) [17]. Brownlee has proposed that

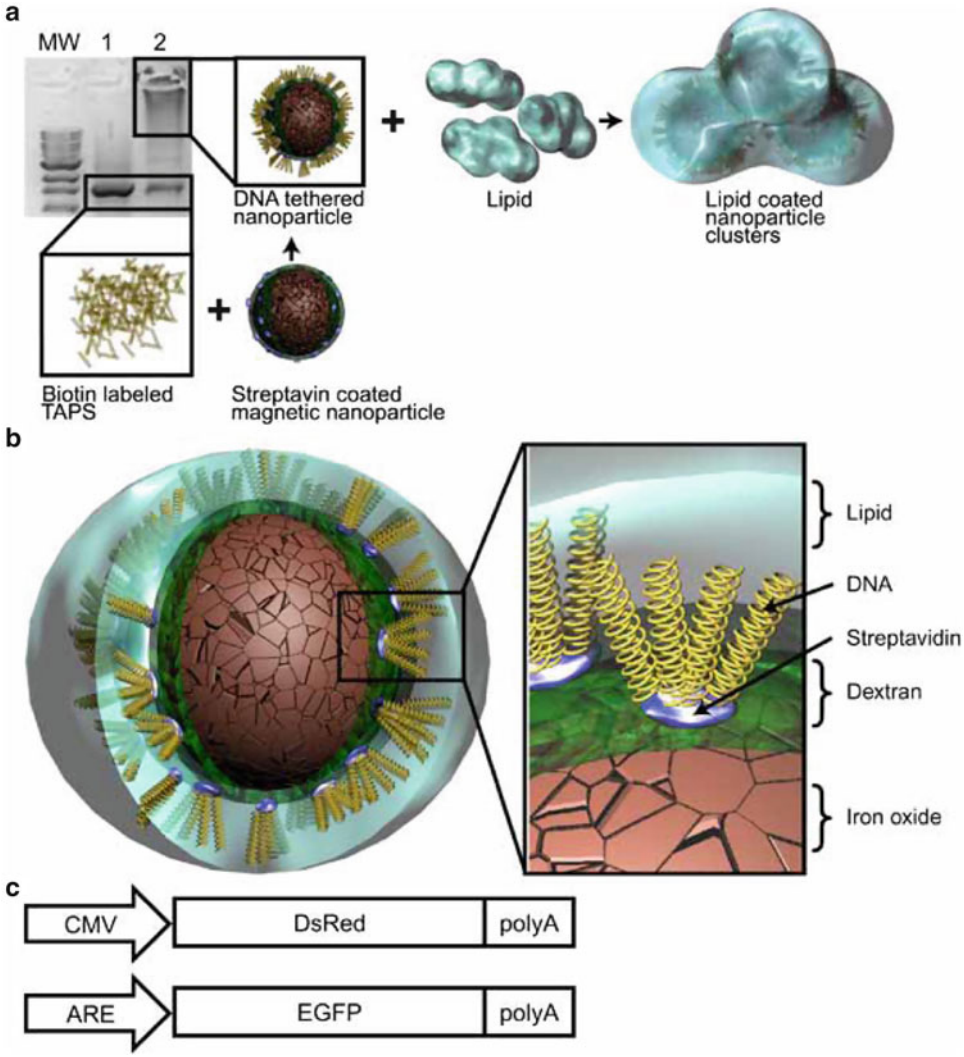

Fig. 2 (**a**) Schematic of the construction of the MNP. (**b**) The layered anatomy of a lipid coated DNA-tethered nanoparticle. (**c**) Schematics of the two DNA constructs used to assess transfection and ARE activity (Prow et al. (2006) Mol Vis;12:616–625)

the major molecular mechanism in diabetic vascular injury is hyperglycemia-induced process of overproduction of the ROS superoxide by the mitochondrial electron transport chain [18]. In AMD, oxidative stress occurs in the retinal pigment epithelium (RPE) resulting in death of RPE and ultimately photoreceptors.

Oxidative stress is an induced state whose levels are communicated through signalling pathways resulting in the induction of antioxidant genes as a protective measure in cells [19–21]. These responses are coordinated through a complex signalling network involving the ARE [22, 23]. Recently, ARE-based sensors have been developed that are capable of initiating reporter gene

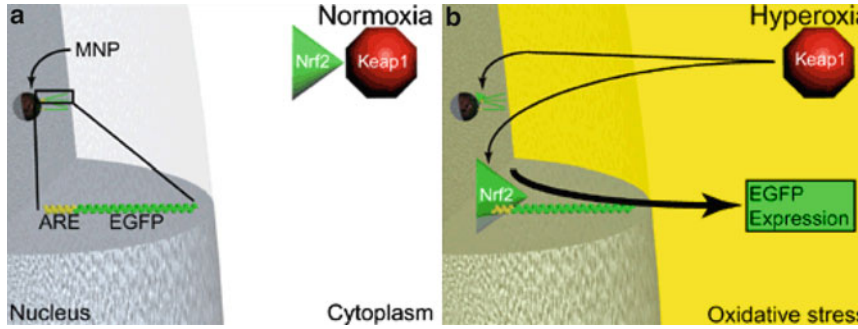

Fig. 3 Normoxia (**a**) and hyperoxia (**b**) influence on transcription of EGFP attached gene (Prow et al. (2006) Mol Vis;12:616–625)

expression in response to the presence of oxidative stress inducing chemicals [22–26].

The ARE is composed of a *cis*-acting enhancer region that is directly controlled by several factors that include the transcription factor Nrf2, a repressor Keap1, and small Maf proteins. Oxidative stress stimulates the dissociation of Keap1 protein from Nrf2 in the cytoplasm [27]. Nrf2 then undergoes nuclear translocation and binding to ARE (illustrated in Fig. 4). The activated ARE enhances the expression of any gene downstream of its sequence. Although the ARE can induce a variety of antioxidant and supporting genes, the literature has repeatedly focused on glutathione s-transferase and NAD(P)H:quinone oxidoreductases [28, 29].

The ROS-induced biosensor is a promoter-based system that relies on cellular machinery for the detection of ROS. The cell detects ROS and activates transcription factors, which bind to specific promoter regions. Transcription downstream of these response elements, in this case a fluorescent reporter gene, is then activated. This construct is composed of a number of ARE repeats followed by a minimal thymidine kinase promoter, ahead of a reporter gene, which enhanced green fluorescent protein or EGFP. The sensitivity of the biosensor is dramatically affected by the number of ARE repeats [24, 25].

The MNP-ARE described herein utilizes a fluorescent reporter protein, EGFP, and the transcriptionally active DNA construct is bound to MNP to detect the cellular response to oxidative stress (Fig. 5). We have used this ARE-tethered nanoparticle to detect oxidative stress from hyperglycemia in vitro and in RPE in the diabetic eyes of rats [12]. This biosensor system has the potential to detect oxidative stress in many disease states and could be used to induce expression of an antioxidant transgene placed in tandem with the ARE sequence when oxidative stress is sensed, i.e., provide antioxidant only when oxidative stress occurs.

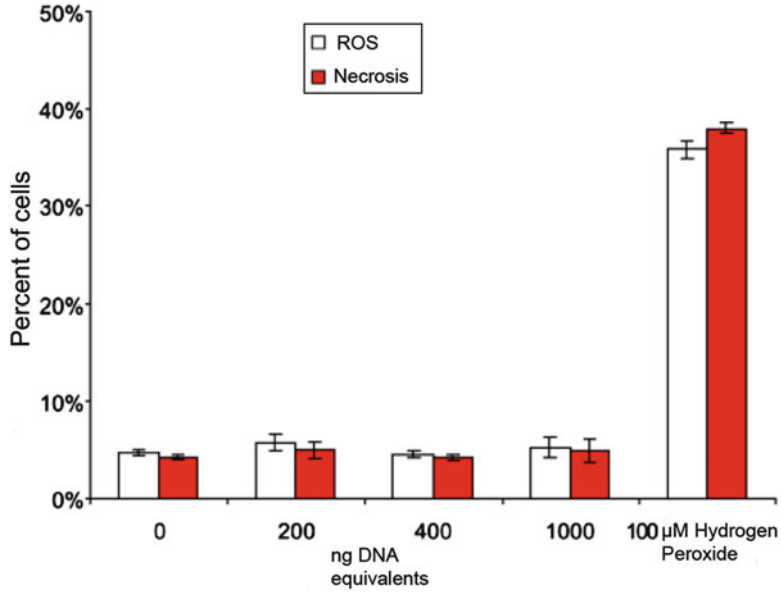

Fig. 4 Uncoated magnetic nanoparticles ability to induce ROS formation or necrosis. Hydrogen peroxide was used as a positive control (Prow et al. (2006) Mol Vis;12:606–615)

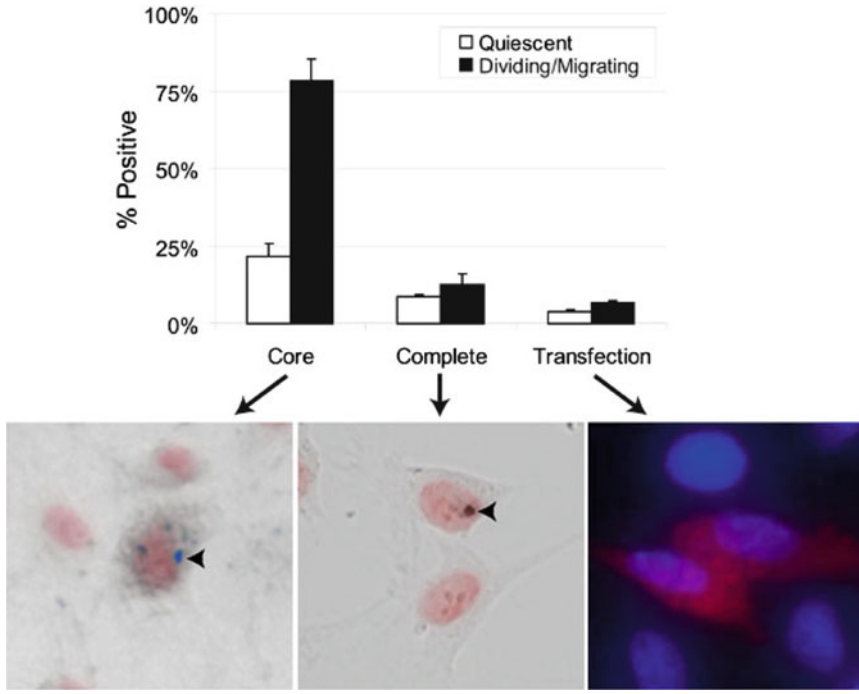

Fig. 5 The presence of magnetic nanoparticle components in transfected cells is indicated by arrowheads (Prow et al. (2006) Mol Vis;12:616–625)

2 Materials

2.1 Equipment

2.1.1 Fluorescence Microscopy

1. Imaging is easiest with a Nikon Eclipse TE2000-U (Nikon, Inc., Melville, NY) inverted fluorescence or a Zeiss 510 META (Carl Zeiss MicroImaging, Inc., Thornwood, NY) confocal microscope. Both UV and 488 nm excitation light are needed for visualizing Hoechst 33342-stained nuclei and EGFP fluorescence, respectively. Emission band-pass filters with 420–480 nm and 510–550 nm ranges will be needed for Hoechst 33342 and EGFP fluorescence imaging, respectively. Light microscopy and fluorescence images can then be overlayed.

2.1.2 Fluorescence Microscopy for ARE-GFP Assessment

1. Confocal analysis can be done with a Zeiss 510 META confocal microscope (Carl Zeiss MicroImaging, Inc., Thornwood, NY).
2. Set the excitation wavelengths to include 405 and 488 nm for Hoechst 33342 and EGFP, respectively.
3. The laser powers are set to 10 % and 5 % for the 405 nm and 488 nm lasers, respectively.
4. Set the emission filters to 420–480 nm emission bandpass for Hoechst 33342 and 510–550 nm emission bandpass for EGFP.
5. The objective can be set to 5, 10, 20, 40, 63, or 100×.
6. Take images in the plane of the nuclear fluorescence from the Hoechst 33342 in order to assure that the images contain cellular bodies, *see* **Note 3**.

2.2 PCR Reagents

1. Oligonucleotide primers for the PCR amplification of the ARE promoter and the EGFP reporter with a biotin label on the 5′ terminus of the forward primer (Integrated DNA Technologies, Coralville, Iowa, USA).
2. pARE-EGFP for the PCR template (William Fahl, University of Wisconsin, Madison, WI, USA and Ming Zhu, Arizona Cancer Center, Tuscon, AZ, USA).
3. Taq, PCR butter, dNTPs, agarose, ethidium bromide, Tris, glacial acetic acid, EDTA, and molecular grade water (Sigma Chemicals, Inc., St. Louis, MO).
4. PCR tubes, thermocycler, gel casting tray, DNA size marker and UV transilluminator (Thermo Fisher Scientific, Inc., Pittsburgh, PA, USA).

2.3 Magnetic Nanoparticles

1. Superparamagnetic nanoparticles coated with streptavidin, magnetic columns, and equilibration buffer (Miltenyi Biotec, Auburn, CA).

2.4 Cell Culture, Transfection, and Fixation Reagents

1. Opti-MEM®, Lipofectamine™ 2000, trypsin, DMEM/F12, fetal bovine serum (FBS) from Invitrogen, Carlsbad, CA, USA.
2. Tissue culture flasks and chamber slides (Thermo Fisher Scientific, Inc., Pittsburgh, PA, USA).
3. Hoechst 33342 is a nuclear counterstain dye (Sigma-Aldrich, St. Louis, MO, USA).
4. Paraformaldehyde, Triton-X, and Tris-buffered saline (TBS) are used to fix, permeabilize, and rinse the treated cells (Sigma-Aldrich, St. Louis, MO, USA).

2.5 Prussian Blue Staining Reagents

Hydrochloric acid and potassium ferrocyanide can both be purchased from Sigma-Aldrich, St. Louis, MO, USA.

3 Methods

3.1 Preparation of Biotin-Labeled Transcriptionally Active PCR Products

1. Combine the following components on ice to make a master PCR mix:
   (a) Forward primer (5′-TAG TTA TTA ATA GTA ATC-3′) at 20 μM or 20 μL.
   (b) Reverse primer (5′-TAC ATT GAT GAG TTT GGA-3′) at 20 μM or 20 μL.
   (c) Template at 10 ng/μL 10 μL.
   (d) Taq at 1.5 units per reaction × 20 reactions 10 μL.
   (e) 10× buffer 100 μL.
   (f) dNTPs 20 μL.
   (g) H_2O 820 μL.
2. Mix the master mix thoroughly and then aliquot the mix into 9 PCR tubes at 100 μL per tube and the balance in a final tube.
3. Cap tubes and put them into the thermocycler to run the PCR.
4. PCR temperature profile:
   (a) Denaturation at 94 °C for 2 min.
   (b) Denaturation at 94 °C for 30 s (35 cycles of **steps b–d**).
   (c) Annealing at 53 °C for 30 s.
   (d) Extension at 72 °C for 2 min.
   (e) Final extension at 72 °C for 6 min.
   (f) Store at 4 °C until ready to run the gel.
5. Weigh out agarose to make a 1 % gel in a total volume of 25 mL (0.25 g) in Tris-acetic acid-EDTA buffer (TAE). Add 25 mL of buffer and heat agarose until dissolved. Let the gel sit until the gel cools slightly. Add ethidium bromide to a final concentration of 0.5 μg/mL and pour the gel.
6. Set up gel in the gel casting apparatus. Place the comb.

7. Pour the gel into the gel tray and ensure there are no air bubbles in the gel or on the comb.
8. Allow to cool (about 10 min), then fill the electrophoresis chamber with TAE.
9. Mix 5 μL of PCR product with 2 μL of gel loading dye.
10. Load 5 μL of PCR product.
11. Load 5 μL of DNA 1 kb ladder.
12. Run gel at 100 V for 30 min.
13. Visualize bands with a UV transilluminator. The expected product size is 2 kb.

3.2 DNA-Tethered Nanoparticle Construction

1. Quantitate the amount of purified PCR product you purified on the previous day using a spectrophotometer.
2. Incubate the magnetic nanoparticles with the biotin-labeled PCR fragments at ~30 ng of PCR product per 1 μL of nanoparticle solution. Use 1 μg of DNA combined with 33 μL of magnetic nanoparticles.
3. Incubate the mixture at room temperature for 30 min.
4. During this time, prepare the magnetic column by equilibrating with 50 μL of equilibration buffer. Add all solutions directly to the center of the column.
5. Wash the column once with 100 μL Opti-MEM®.
6. Load the column with the DNA/nanoparticle mixture.
7. Wash the column three times with 100 μL Opti-MEM®.
8. Elute the nanoparticles by removing the column from the magnet and adding 100 μL of Opti-MEM®. Allow the column to gravity drain into a sterile tube.
9. Coat the DNA-labeled magnetic nanoparticles with lipid (Lipofectamine™ 2000).
   (a) Add 1 μL of Lipofectamine™ 2000 to 100 μL of Opti-MEM®. Gently mix by tapping the side of the tube. Do not vortex. Let the solution stand at room temperature for 5 min, *see* **Note 1**.
   (b) Add the eluted nanoparticles drop by drop to the center of the Opti-MEM® Lipofectamine™ 2000 solution. Gently mix by tapping the side of the tube. Let the solution stand at room temperature for 20 min before transfection onto cell culture (4-well chamber slide).

3.3 Cell Culture for In Vitro Transfection

1. Remove the media from the flask and wash the cells with PBS. Remove the PBS and discard.
2. Add 0.5 mL of trypsin to a T25 flask of cells. Place at 37 °C for 5 min.

3. Dislodge cell with gentle tapping on the side of the flask.
4. Quench the trypsin with 5 mL of DMEM/F12 10 % FBS.
5. Resuspend the cells by gentle pipetting up and down until the mixture is homogenous.
6. Determine cell density with a Neubauer chamber.
7. Prepare a 10 mL cell suspension of 40,000 cells/mL in DMEM/F12 w/10 % FBS.
8. Add 1 mL of cell suspension in a random pattern to each well in a 4-well chamber slide, for example.

3.4 In Vitro Transfection

1. Check the chamber slides to ensure the cells are viable and healthy.
2. Label chamber slides with the following:
   (a) Negative control—Opti-MEM® only + Lipofectamine™ 2000.
   (b) Plasmid control—Plasmid only + Lipofectamine™ 2000.
   (c) PCR control—purified biotin-labeled PCR product + Lipofectamine™ 2000.
   (d) Complete magnetic nanoparticles + Lipofectamine™ 2000.
3. Add 400 μL of Opti-MEM® to a microfuge tube plus 4 μL of Lipofectamine™ 2000. Gently mix by tapping the side of the tube. Do not vortex. Let the tube stand at room temperature for 5 min.
4. Prepare transfection solutions for the four wells in sterile tubes:
   (a) 100 μL of Opti-MEM®.
   (b) 100 μL of Plasmid (already diluted so the final concentration added to cells will be 1 μg).
   (c) Dilute purified PCR product in 100 μL, for a total of 1 μg, of Opti-MEM®.
5. After a 5 min incubation, add 100 μL of the Opti-MEM®/Lipofectamine™ 2000 solution to each of the transfection solutions, **steps 2a–c**. Gently mix by tapping the tube. Add the complete MNP solution from Subheading 3.2 to the well for the **step 2d** group.
6. Remove media from all wells of the chamber slide.
7. Wash with 1 mL of Opti-MEM® to remove any traces of antibiotics from the media.
8. Add 200 μL of each transfection solution to the corresponding wells and incubate the chamber slides at 37 °C for 1 h. Gently shake the chamber slides every 15 min for 1 h.
9. Remove the transfection solutions and wash the cells with 1 mL of Opti-MEM®.

10. Remove Opti-MEM® and replace with 1 mL of complete media (DMEM/F12 with 10 % FBS).
11. Incubate chamber slides at 37 °C overnight.

3.5 Prussian Blue Staining to Visualize Iron Nanoparticles

Prussian blue staining is used to detect cells that contain magnetic nanoparticles. This staining protocol detects nanoscale iron oxide crystals particles. Therefore, this procedure does not imply that the cells contain complete magnetic particles, just the iron oxide core of the nanoparticle.

1. The cells are fixed and permeabilized using 2 % paraformaldehyde and permeabilized with 0.25 % Triton-X.
2. Remove media from all wells of the chamber slide.
3. Add 0.5 mL of 2 % paraformaldehyde in Tris-buffered saline pH 7 (TBS) for 10 min at room temperature.
4. Remove paraformaldehyde and discard.
5. Permeabilize cells by the addition of 0.5 mL of 0.25 % Triton-X 100 in TBS for 10 min at room temperature.
6. Remove and discard Triton solution.
7. Counterstain cells with a 20,000 dilution (i.e., 1 μL in 20 mL of PBS) of Hoechst 33342. Add 0.5 mL per well and incubate for 15 min in the dark at room temperature.
8. Remove Hoechst stain and discard. Wash cells with 0.5 mL of PBS, three times.
9. After the final wash, leave the PBS in the wells.
10. Make a fresh staining solution containing equal parts of 20 % hydrochloric acid and 10 % potassium ferrocyanide.
11. Remove the PBS from the cells and add 0.5 mL of the staining solution. Incubate for 20 min at room temperature.
12. Wash cells three times with 0.5 mL of PBS.
13. Leave the PBS in the well and visualize cells, *see* **Note 2**.

4 Notes

1. The amount of lipid needs to be balanced by the toxicity profile in the cells or tissue and the potential for increases in transfection efficiency.
2. Positive reactions generally occur promptly and look like blue spots within the cell. These blue spots are the result of the ferric iron in the nanoparticle combined with the potassium ferrocyanide to form ferric-ferrocyanide, which has a bright blue color. Viewing the cells or tissue section with a bright light for prolonged time can cause a false-positive reaction.

3. The zoom, objective, brightness, contrast, laser power, and gain must remain the same for all groups and images to enable comparisons to be made.

5 Conclusions

The use of a synthetic signalling pathway to noninvasively study the progression of disease and therapeutic interventions could facilitate the development of better therapeutics for a number of diseases. There are a large number of diseases with ROS components, yet studying ROS during disease progression has remained a significant challenge. We developed a magnetic nanoparticle biosensor that can report cellular responses to oxidative stress via fluorescent proteins. This technology enables researchers to monitor, in real time, ROS responses with noninvasive microscopy. This is useful, for example, in monitoring microvascular diseases with ROS components, e.g., diabetic retinopathy (*see* Figs. 4 and 5). Microvascular disease is implicated in the etiology of diabetic complications in most organ systems. It is unclear if loss in viable microvasculature is due to toxicity of the hyperglycemic state or actual occlusive events caused circulating cells or substances. It is likely that both toxicity and occlusions play a role in diabetic complications and these effects are initiated through the metabolic hallmark of diabetes, hyperglycemia. Hyperglycemia is a cause of pancreatic beta cell loss and also activates peripheral blood mononuclear cells (PBMC) and endothelial cells. At the source of these pathogenic processes is hyperglycemia-induced mitochondrial oxidative stress (MOS). To understand how we can treat MOS in diabetes, we must better understand the cellular responses to the hyperglycemic state and define the best strategies for the treatment of MOS. Using systems like our nanobiosensor for ROS can enable researchers to ask the following questions in the context of animal models of diabetes: How does MOS affect the major antioxidant promoters? What are the best mitochondrial-targeted antioxidant therapies for treating MOS? Can synthetic or natural antioxidant promoters that are sensitive to MOS be used as biosensors to switch on and off the expression of mitochondrial-targeted antioxidant enzymes?

References

1. Lin L, Grice JE, Butler MK et al (2011) Time-correlated single photon counting for simultaneous monitoring of zinc oxide nanoparticles and NAD(P)H in intact and barrier disrupted volunteer skin. Pharm Res 28(11):2920–2930
2. Monteiro-Riviere NA, Wiench K, Landsiedel R, Schulte S, Inman AO, Riviere JE (2011) Safety evaluation of sunscreen formulations containing titanium dioxide and zinc oxide nanoparticles in UVB sunburned skin: an in vitro and in vivo study. Toxicol Sci 123(1):264–280
3. Violante MR (1990) Potential of microparticles for diagnostic tracer imaging. Acta Radiol Suppl 374:153–156

4. Bernd H, De Kerviler E, Gaillard S, Bonnemain B (2009) Safety and tolerability of ultrasmall superparamagnetic iron oxide contrast agent: comprehensive analysis of a clinical development program. Invest Radiol 44:336–342
5. Mahmoudi M, Hosseinkhani H, Hosseinkhani M et al (2011) Magnetic resonance imaging tracking of stem cells in vivo using iron oxide nanoparticles as a tool for the advancement of clinical regenerative medicine. Chem Rev 111:253–280
6. Grutzkau A, Radbruch A (2010) Small but mighty: how the MACS-technology based on nanosized superparamagnetic particles has helped to analyze the immune system within the last 20 years. Cytometry A 77:643–647
7. Prow TW, Kotov NA, Lvov YM, Rijnbrand R, Leary JF (2004) Nanoparticles, molecular biosensors, and multispectral confocal microscopy. J Mol Histol 35:555–564
8. Prow T, Grebe R, Merges C et al (2006) Nanoparticle tethered antioxidant response element as a biosensor for oxygen induced toxicity in retinal endothelial cells. Mol Vis 12: 616–625
9. Prow T, Smith JN, Grebe R et al (2006) Construction, gene delivery, and expression of DNA tethered nanoparticles. Mol Vis 12: 606–615
10. Prow TW (2010) Toxicity of nanomaterials to the eye. Wiley Interdiscip Rev Nanomed Nanobiotechnol 2:317–333
11. Prow TW, Bhutto I, Kim SY et al (2008) Ocular nanoparticle toxicity and transfection of the retina and retinal pigment epithelium. Nanomedicine 4:340–349
12. Prow TW, Bhutto I, Grebe R et al (2008) Nanoparticle-delivered biosensor for reactive oxygen species in diabetes. Vision Res 48:478–485
13. Bergua A, Mayer B, Neuhuber WL (1996) Nitrergic and VIPergic neurons in the choroid and ciliary ganglion of the duck Anis carina. Anat Embryol (Berl) 193:239–248
14. Brownlee M (2003) A radical explanation for glucose-induced beta cell dysfunction. J Clin Invest 112:1788–1790
15. Giardino I, Edelstein D, Brownlee M (1996) BCL-2 expression or antioxidants prevent hyperglycemia-induced formation of intracellular advanced glycation endproducts in bovine endothelial cells. J Clin Invest 97:1422–1428
16. Wiernsperger NF (2003) Oxidative stress as a therapeutic target in diabetes: revisiting the controversy. Diabetes Metab 29:579–585
17. Beatty S, Koh H, Phil M, Henson D, Boulton M (2000) The role of oxidative stress in the pathogenesis of age-related macular degeneration. Surv Ophthalmol 45:115–134
18. Brownlee M (2001) Biochemistry and molecular cell biology of diabetic complications. Nature 414:813–820
19. Cory JG, Szentivanyi A (1987) Cancer biology and therapeutics. Plenum, New York
20. Prochaska HJ, De Long MJ, Talalay P (1985) On the mechanisms of induction of cancer-protective enzymes: a unifying proposal. Proc Natl Acad Sci USA 82:8232–8236
21. Prochaska HJ, Talalay P (1988) Regulatory mechanisms of monofunctional and bifunctional anticarcinogenic enzyme inducers in murine liver. Cancer Res 48:4776–4782
22. Friling RS, Bergelson S, Daniel V (1992) Two adjacent AP-1-like binding sites form the electrophile-responsive element of the murine glutathione S-transferase Ya subunit gene. Proc Natl Acad Sci USA 89:668–672
23. Wasserman WW, Fahl WE (1997) Functional antioxidant responsive elements. Proc Natl Acad Sci USA 94:5361–5366
24. Zhu M, Fahl WE (2000) Development of a green fluorescent protein microplate assay for the screening of chemopreventive agents. Anal Biochem 287:210–217
25. Zhu M, Fahl WE (2001) Functional characterization of transcription regulators that interact with the electrophile response element. Biochem Biophys Res Commun 289: 212–219
26. Zhu M, Chapman WG, Oberley MJ, Wasserman WW, Fahl WE (2001) Polymorphic electrophile response elements in the mouse glutathione S-transferase GSTa1 gene that confer increased induction. Cancer Lett 164: 113–118
27. Dinkova-Kostova AT, Holtzclaw WD, Cole RN et al (2002) Direct evidence that sulfhydryl groups of Keap1 are the sensors regulating induction of phase 2 enzymes that protect against carcinogens and oxidants. Proc Natl Acad Sci USA 99:11908–11913
28. Day RM, Suzuki YJ, Fanburg BL (2003) Regulation of glutathione by oxidative stress in bovine pulmonary artery endothelial cells. Antioxid Redox Signal 5:699–704
29. Jaiswal AK (2000) Regulation of genes encoding NAD(P)H:quinone oxidoreductases. Free Radic Biol Med 29:254–262